Persistent Ground-State Planar Alignment of Iodine Molecule through Resonant Excitation

M. Bournazel, A. Espaignol, D. Singh, R. K. Bhalavi, F. Billard, P. Béjot, E. Hertz, O. Faucher

Persistent ground-state planar alignment of iodine molecule through resonant excitation

M. Bournazel, A. Espaignol, D. Singh, R. K. Bhalavi, F. Billard, P. Béjot, E. Hertz, and O. Faucher[1*]
[1] *Laboratoire Interdisciplinaire CARNOT de Bourgogne, UMR 6303 CNRS-Université de Bourgogne, BP 47870, 21078 Dijon, France*
(Dated: September 25, 2024)

We demonstrate the generation of a persistent planar molecular alignment by subjecting a relatively warm gas sample to a resonant femtosecond laser pulse. By optically probing I_2 molecules in their vibronic ground states, we observe a persistent delocalization of their axes near the plane orthogonal to the field direction. This phenomenon is attributed to the one-photon resonant excitation, primarily removing molecules from the thermal ground state distribution that are initially aligned along the field, i.e. those with small projection of their rotational angular momentum along the field.

PACS numbers: 37.10.Vz, 45.50.Hz, 42.50.Md

The concept of using a strong laser pulse to align molecules [1–3] in space gained significance with the advent of the first experiments in the early nineties (see, e.g., [4–8]). Since then, substantial efforts have been dedicated to improving our understanding of the underlying physics and pushing back experimental limits. In the quest for a better control over the process, successful studies have demonstrated the influence of various experimental factors (for a review see [9, 10]), including the pulse parameters of the applied field, the temperature of the system, and the environmental conditions, such as molecules trapped in nano droplets [11, 12], molecular rotors in bulk superfluid [13], or molecules exposed to collisions [14, 15]. While most of these studies have focused on molecules non resonantly coupled to a laser field through their polarizability, molecules aligned through resonant optical field interactions have received comparatively little attention. In [3], one of the earliest theoretical works on molecular alignment in intense laser fields, T. Seideman considers the role of an electronic resonance to improve alignment of I_2 and LiH. The present work reports the experimental observation of laser induced molecular alignment achieved through the resonant excitation of an electronic state. We show that the excitation of several rovibronic transitions of warm I_2 molecules by a single laser pulse, linearly polarized, leads to a persistent planar alignment [16] of the molecules in the azimuthal plane. To the best of our knowledge, only one experiment has reported persistent planar alignment [17], also termed anti-alignment, of a linear molecule. This has been achieved using two crossed-polarized laser fields leading to a delocalization of the molecule in the plane perpendicular to the propagation direction of the fields. In contrast to the findings of [17], the resonant excitation explored in the present work results in a persistent anti-alignment formed within the plane perpendicular to the polarization direction of the field. The effect is particularly robust to thermal averaging, rendering it highly suitable for various potential applications.

To resonantly align iodine molecules, we employ a tunable ~ 100 fs pump radiation generated by a non-collinear parametric amplifier (NOPA). In summary, a linearly polarized pump pulse is focused into an iodine vapor cell. At the focal point, the pump pulse is overlapped with a 400 nm time-delayed nonresonant weak probe pulse polarized at 45° with respect to the polarization direction of the pump field. The alignment of the molecules affects the refractive index of the gas through the Kerr effect. The resulting birefringence experienced by the probe beam is measured with a balanced-photodetection system, producing a signal proportional to the thermal average of $\left(\langle\cos^2\theta\rangle(\tau) - 1/3\right)$, where θ is the angle between the molecular axis and the direction of polarization of the pump field, τ is the pump-probe delay, and 1/3 is the expectation value $\langle\cos^2\theta\rangle(\tau)$ for randomly oriented molecules.

The alignment signal depicted in Fig. 1 (a) has been observed by tuning the wavelength generated by the NOPA system to $\lambda = 568$ nm. This wavelength resides within the spectral region of the $B(^3\Pi_u^+)-X(^1\Sigma_g^+)$ parallel transition where the one-photon resonances contribute to the largest alignment signal. As expected for a homopolar diatomic molecule, the signal exhibits a distinct pattern featuring four revivals occurring within a rotational period. The right vertical axis provides the value of the alignment factor $(\langle\langle\cos^2\theta\rangle\rangle_T(t) - 1/3)$ (see its definition further bellow), which has been obtained by calibrating the alignment signal of I_2, using CO_2 as a reference molecule. For the estimated gas cell temperature $T \sim 425$ K, three vibrational levels of the ground electronic state, $v" = 0$, 1, and 2, are predominantly populated. Each of them presents a quite similar rotational structure, with a constant of rotation $B_{v"} \simeq 0.37$ cm^{-1} [18], leading to an averaged rotational period of the ground state wavepacket $T_R = \pi\hbar/B_{v"} \simeq 448$ ps, consistent with the observation. Beside the overall revival signature, the most striking feature disclosed by

* olivier.faucher@u-bourgogne.fr

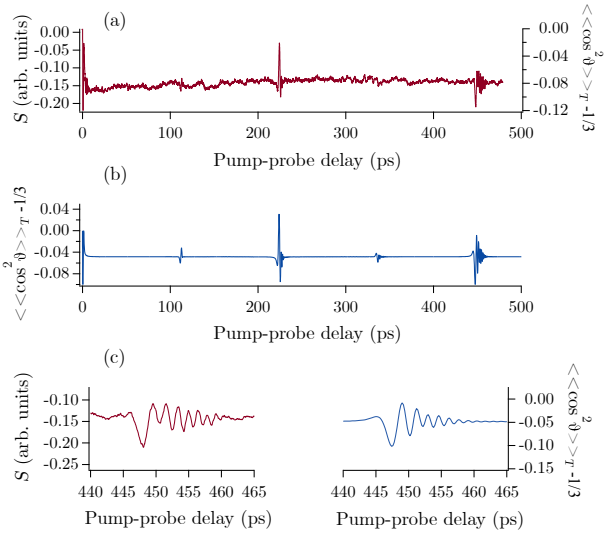

FIG. 1. (a) Alignment signal S induced by a pump pulse (peak intensity $I \approx 10\,\mathrm{TW/cm^2}$) one-photon resonant with the $B-X$ electronic transition of iodine molecule. The right ordinate axis gives the calibrated value of $(\langle\langle\cos^2\theta\rangle\rangle_T(t) - 1/3)$ estimated with a relative uncertainty of $\pm 20\%$. (b) Calculated ground state alignment factor. (c) Measured (left) and calculated (right) fourth alignment revival.

the measured signal concerns its large negative time-average value, which reveals a persistent molecular anti-alignment phenomenon occurring within the plane perpendicular to the polarization of the exciting field. To elucidate the origin of the observed effect, we have developed a numerical model for resonantly induced molecular alignment incorporating vibronic couplings between the X and B electronic state.

The quantum dynamics is described by solving the Liouville-von Neumann equation

$$\partial_t \rho(t) = -\frac{i}{\hbar}\left[H_0 + H_L(t), \rho(t)\right], \tag{1}$$

where $\rho(t)$ is the density operator, H_0 is the field-free Hamiltonian of the system, $[\ ,\ ]$ denotes a commutator, and

$$H_L(t) = -\frac{1}{2}\mathcal{E}_\mathrm{p}(t)\mu_e \cos\theta \tag{2}$$

describes the coupling of the system to the linearly polarized laser pump field $\mathcal{E}_\mathrm{p}(t)$, via the electric field induced dipole μ_e, considering a parallel transition. Note that due to the low number density of molecules in the experiment, dissipation terms are neglected in the model, as well as the hyper-fine structure of the molecule leading to a decrease of the revivals versus time, as reported for low temperature ($T \sim 0.8\,\mathrm{K}$) iodine molecules aligned by a 800 nm laser pulse [19]. Under the Born-Oppenheimer and R-centroid approximation, the matrix element of the dipole moment between the lower ψ'' and upper state ψ' is given by

$$\langle\psi'|\,\mu_e\cos\theta\,|\psi''\rangle = \mu_e(\overline{R})\,\langle v'|v''\rangle\,\langle J'M'|\cos\theta\,|J''M''\rangle\,, \tag{3}$$

where $\mu_e(\overline{R})$ is evaluated at the R-centroid and $|\langle v'|v''\rangle|^2$ is the Franck-Condon factor [20]. Recall that J and M are the quantum numbers associated to the total angular momentum and its projection onto the quantification axis chosen along the pump field polarization, respectively, and v is the quantum of vibration. Due to the large difference in internuclear distances between the ground and electronic state of I_2, $\langle v'|v''\rangle$ spans a wide range of vibrational bands (v',v''). A reasonable convergence of our simulations was achieved by limiting the number of these bands to 27, with v'=16-24 and v''=0-2, and the rotational basis to $J_\mathrm{max} = 200$, leading to a rovibronic basis comprising 241200 $|v, J, M\rangle$ states.

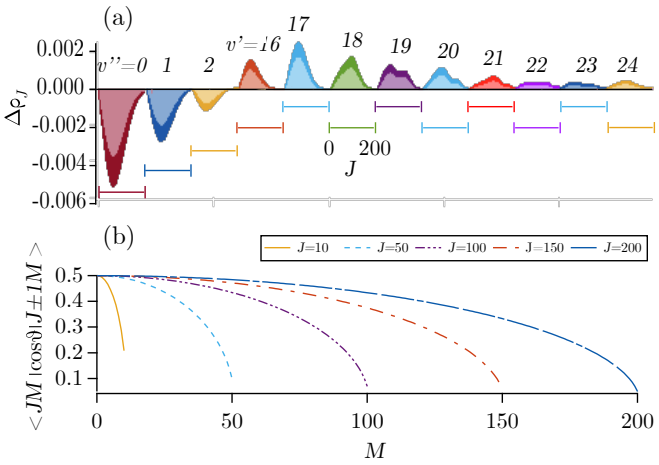

FIG. 2. (a) Rotational population change $\Delta\rho_J = \rho_J(t \gg 0) - \rho_J(t < 0)$ of the system. v'' and v' refer to the vibrational quantum numbers relative to the ground and excited electronic X and B state, respectively. (b) M-dependence of the rotational coupling terms $\langle JM|\cos\theta\,|J \pm 1M\rangle$ depicted for some J values.

The coupling term of Eq. 3 initiates first-order rotational coherences $|J''\rangle\langle J' = J'' \pm 1|$ between the two electronic states, as well as second-order coherences $|J'\rangle\langle J' \pm 2|$ and $|J''\rangle\langle J'' \pm 2|$ within the B and X state, respectively. However, our birefringent detection is only sensitive to this last type of coherences. The latters manifest themselves through the time-dependent component of the observable

$$\langle\langle\cos^2\theta\rangle\rangle_T(t) = \left\langle \frac{\sum_{J_1''M,J_2''M}\rho_{J_1''M,J_2''M}\cos^2\theta_{J_2''M,J_1''M}}{\sum_{J_1''M}\rho_{J_1''M,J_1''M}}\right\rangle_T, \tag{4}$$

where $J_2'' - J_1'' = 0, \pm 2$. In this expression, $\rho_{J''M,J''M} = \langle J''M|\,\rho\,|J''M\rangle$ and $\rho_{J''M,J''\pm 2M} = \langle J'' \pm 2M|\,\rho\,|J''M\rangle$ are the populations and second-order rotational coherences of the X state, respectively, and $\langle\rangle_T$ denotes the averaging over the initial thermal distribution of

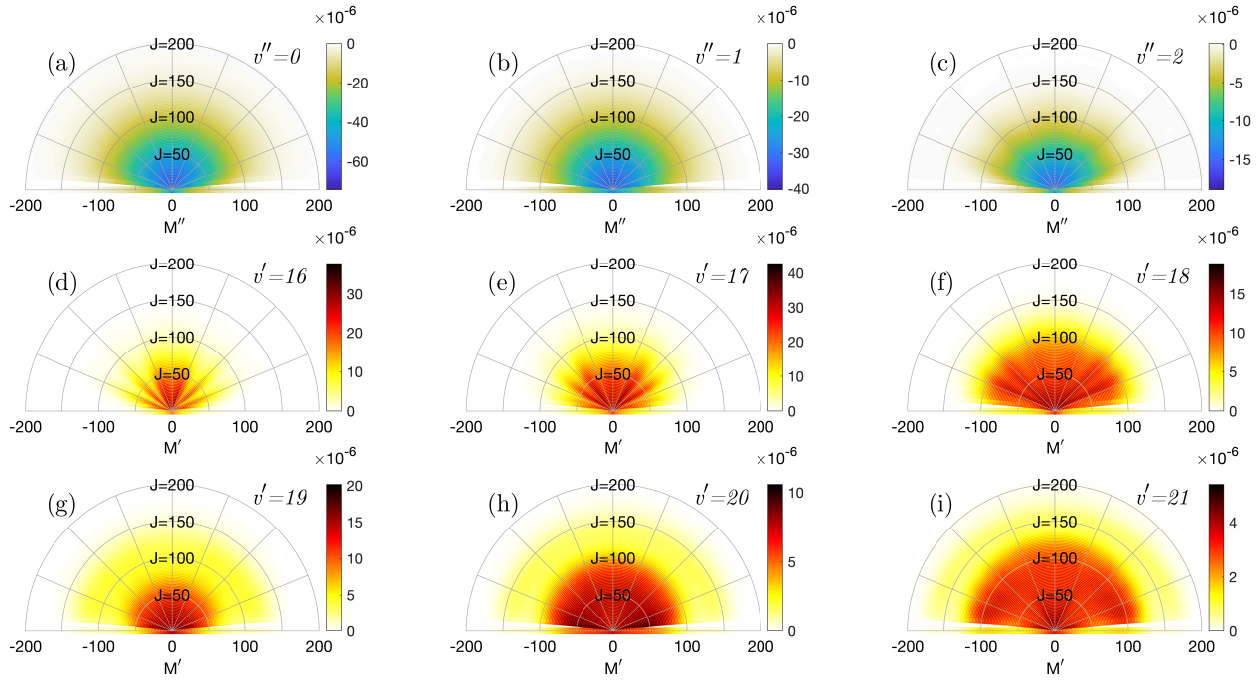

FIG. 3. Relative variation $\Delta\rho_{JM}$ of the M-state populations for the different rovibronic levels of the (a)-(c) ground and (d)-(i) excited electronic state. The population distribution of the $v' = 22 - 24$ states are not shown so as not to overload the figure. The plot discontinuities in the vicinity of $|M/J| = 1$ result from the quantization of M.

populations considering the different statistical weights of the nuclear spin isomers. The alignment factor $(\langle\langle\cos^2\theta\rangle\rangle_T(t) - 1/3)$, calculated from the dipole moments and Franck-Condon factors given in Refs. [20, 21], is shown in Figs. 1(b) and 1(c). Note the relatively good agreement between measurement and calculation, not only regarding to the temporal variation of the signal, but also with respect to the calibrated value of the signal.

Before commenting on the revivals, we first focus on the presence of a significative negative mean value, $(\langle\langle\cos^2\theta\rangle\rangle_T - 1/3 \simeq -0.05)$, which confirms the experimental observation presented in Fig. 1 (a). To provide an approximate scale of the observed effect, consider that this value, disregarding its sign, is comparable to the persistent alignment achievable by exposing room temperature CO_2 molecules to a 800 nm pulse of peak intensity 80 TW/cm^2. The origin of the effect can be explained by inspecting the states of the system excited by the aligning pulse. Figure 2 (a) shows the variation of the rovibronic J-state population calculated after the pump pulse turnoff. As expected, the resonant interaction results in the depletion of all ground vibronic state populations ($\Delta\rho_J < 0$) in favor of the vibrational levels ($\Delta\rho_J > 0$) of the B state. It is interesting to analyse how the angular momentum $\mathbf{J}$ of the molecule is affected by the pump by looking at the M-subspace population in each J state. Let us first recall that the interaction of the system with a linearly polarized field conserves the projection M of $\mathbf{J}$ along the direction of polarization. Figure 2 (b) depicts the rotational dependence $\langle J \pm 1M|\cos\theta\,|JM\rangle$ of Eq. 3 obtained by neglecting the spin and angular momentum of the electronic excited state [22]. As indicated, the amplitude of a $J \to J \pm 1$ transition is all the more important as M is small compared to J, and is maximum for $M = 0$. This can be interpreted by the fact that it is easier to excite a molecule when it is aligned along the field, i.e. a molecule in a $M \ll J$ state. It is therefore expected that the pump pulse primarily depletes the ground vibronic levels from their most aligned $M'' \ll J''$ rotational states promoting the system to the different vibrational levels of the B state. In order to support this argument, we have calculated the populations of the $|JM\rangle$ states after interaction with the pump field and depicted their variation $\Delta\rho_{JM}$ in Fig. 3. For the sake of clarity, $\Delta\rho_{JM}$ is depicted using polar coordinates, where the radius and the angle are associated to J and $\arccos(M/J)$, respectively. The general observation is that, for the ground electronic state, the depletion of the rovibronic populations is more pronounced for $|J''M''\rangle$ states with $M'' \ll J''$, which translates in Figs. 3(a)-3(c) by a $\Delta\rho_{JM}$ distribution exhibiting a petal shape. Conversely, the rotational populations of the vibrational levels in the B state are more pronounced at the edge of the M' state distribution, as shown in Figs. 3(d)-3(i). Note that it cannot be ruled out that multiphoton ionization or dissociation, not included in our model, could also contribute to a persistent

alignment of the ground states.

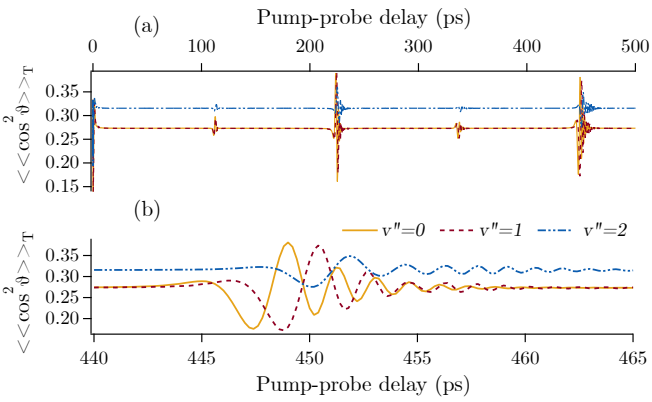

FIG. 4. (a) Alignment factor $\langle\langle\cos^2\theta\rangle\rangle_T(t)$ as a function of the pump-probe delay calculated for the first three vibrational levels $v'' = 0-2$ of the ground electronic state. (b) Enlarged horizontal scale around the fourth revival to illustrate the interference effect between the three levels.

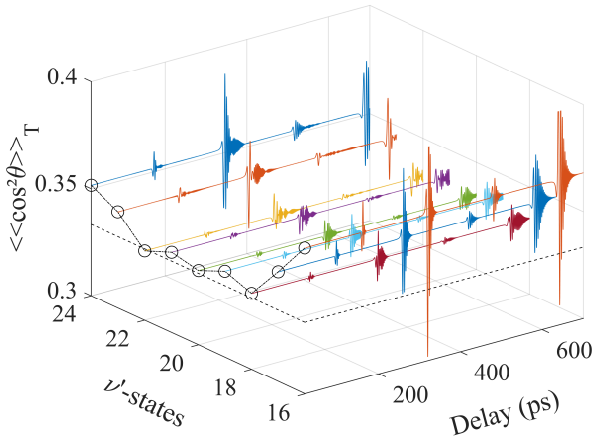

FIG. 5. Calculated alignment factor $\langle\langle\cos^2\theta\rangle\rangle_T(t)$ as a function of the pump-probe delay for the different vibrational levels v' =16-24 of the electronic excited B state. The dash lines (circles) refer to $\langle\langle\cos^2\theta\rangle\rangle_T = 1/3$ (the level of persistent alignment).

The contributions of vibrational levels of the X state to the alignment factor are depicted in Fig. 4 (a). As anticipated from the results of Figs. 3(a)-3(c), all these levels exhibit varying degrees of persistent planar alignment, depending on the strength of their coupling to the vibrational levels of the B state. It has been shown [23] that the slight difference in the rotational constants of the three vibrational levels leads to a dephasing of their respective revivals, which is also observed in our study. As shown in Fig. 4 (b), the sum of the three alignment factors, properly weighted to describe the statistical ensemble of molecules, leads to the observable depicted in Figs. 1(b) and 1(c). The resulting macroscopic interference produces a significant reduction of the revivals, as shown for instance for the fourth revival, where the contributions from states v" = 1 and 2 are out of phase around 448.8 ps. This attenuation effect, together with the one resulting from the centrifugal distortion, explains the relatively small amplitude of the revivals compared to the persistent planar alignment. Note that as a population effect, the persistent component of the alignment factor is not sensitive to the phase of the rovibrational wave-packets [24]. Regarding molecules promoted to the excited B state, the simulations reported in Fig. 5 reveal a significant persistent alignment in all vibronic states with a maximum value $\langle\langle\cos^2\theta\rangle\rangle_T(t) = 0.37$ observed for $v' = 16$. The alignment of the molecules in the excited vibrational states could be measured either by pump-probe laser induced fluorescence, as demonstrated in [25–27] in the context of rotational and vibrational coherence spectroscopy, or by Cold Target Recoil Ion Momentum Spectroscopy [28, 29]. Although all results presented so far have been obtained using a pump wavelength of 568 nm, other wavelengths have been investigated. In addition to variations in the structural aspect of the revivals, illustrated by Figs. 6(a)-6(c), all our measurements clearly demonstrate a persistent planar alignment of the molecules in the ground electronic state. As shown in Fig. 6 (d), the significance of this common feature varies depending on the excitation wavelength.

Before concluding, it is worth noting that, besides generating a persistent planar alignment, the one-photon resonance, as predicted in [3], significantly enhances the alignment of the molecule. Indeed, due to the very low vapor pressure within the gas cell (∼3 mbar) and the pump-probe cross-beam geometry employed in the experiment, which restricts the optical detection to molecules confined within a very small interaction volume, observing the alignment of I_2 at pump wavelength $\lambda = 800$ nm was not possible without stretching the pulse duration to 250 fs and substantially increasing the intensity to 90 TW/cm^2. This limitation is attributed to the relative weakness of the resonance in the near-IR region. Specifically, at 800 nm, the one-photon absorption in I_2 involves hot vibrational bands of the $B-X$ system with $v'' \approx 14$ [30]. These vibrational levels are poorly populated at $T = 425$ K, typically constituting less than 0.002 % of the total population. Consequently, it can be reasonably assumed that the alignment of I_2 at 800 nm takes place in a nonresonant regime. This assumption aligns with the approach taken in [7, 19, 23], where impulsive alignment of the I_2 molecule was measured and successfully compared to theory. The absence of persistent planar alignment in these three works further underscores the significant role played by the electronic resonance in the effect reported in the present study. Finally, note that simulations predict that the planar alignment effect remains relatively robust with respect to temperature, provided the initial thermal distribution of the rotational J

states is sufficiently broad for more details).

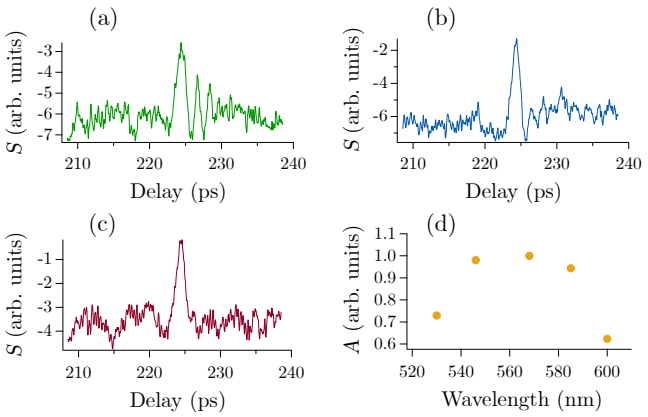

FIG. 6. Second revival of I_2 produced with different wavelengths of the pump laser for the same intensity I=9 TW/cm^2: (a) $\lambda = 530$, (b) 568, and (c) 600 nm. (d) Amplitude A (normalized to unity at $\lambda = 568$ nm) of the second revival versus wavelength.

The results of this letter illustrate the achievement of a significantly persistent planar alignment of a linear molecule through the resonant excitation of an electronic transition. The origin of this effect is attributed to a depopulation process induced by the aligning laser pulse, creating a "dip" in the center of the broad M-state initial distribution associated with each rotational quantum number J of the vibronic ground states. This inhomogeneous distribution is reflected by a complementary "peak" in the M-state pattern of all upper vibronic levels of the excited electronic state coupled to the ground state, resulting in a robust and persistent alignment of the molecule in the excited electronic state. We believe that our findings are pertinent to surface-mediated chemical processes. The challenge of trapping laser-aligned molecules on a surface remains an open and ambitious challenge. One of the practical difficulties related to the observation of such an effect lies in the low-duty cycle of the alignment revivals. A significant degree of persistent anti-alignment, as produced in resonant molecular alignment, would enhance the probability of attaching a molecule to a surface and thus facilitate such experiments. Finally, we hope that this work will stimulate interest for investigating new phenomena related to resonant alignment, considering the different electronic and/or nuclear symmetries of the systems, as well as motivate experiments with molecules aligned in excited electronic states.

ACKNOWLEDGMENTS

M.B. and A.E. contributed equally to this work. The work was supported by the Conseil Régional de Bourgogne Franche-Comté, the EIPHI Graduate School (contract No. "ANR-17-EURE-0002") and has benefited from the facilities of the SMARTLIGHT platform in Bourgogne Franche-Comté (EQUIPEX+ contract No. "ANR-21-ESRE-0040").

[1] B. Friedrich, D. P. Pullman, and D. R. Herschbach, Alignment and orientation of rotationally cool molecules, J. Chem. Phys. **95**, 8118 (1991).
[2] B. Friedrich and D. Herschbach, Alignment and trapping of molecules in intense laser fields, Phys. Rev. Lett. **74**, 4623 (1995).
[3] T. Seideman, Rotational excitation and molecular alignment in intense laser fields, J Chem. Phys. **103**, 7887 (1995).
[4] P. M. Felker, J. S. Baskin, and A. Zewail, Rephasing of collisionless molecular rotationnal coherence in large molecules, Journal of Physics Chemistry **90**, 724 (1986).
[5] D. Normand, L. A. Lompre, and C. Cornaggia, Laser-induced molecular alignment probed by a double-pulse experiment, J. Phys. B **25**, L497 (1992).
[6] J. Ortigoso, M. Rodriguez, M. Gupta, and B. Friedrich, Time evolution of pendular states created by the interaction of molecular polarizability with a pulsed nonresonant laser field, J. Chem. Phys. **110**, 3870 (1999).
[7] F. Rosca-Pruna and M. J. J. Vrakking, Experimental observation of revival structures in picosecond laser-induced alignment of I_2, Phys. Rev. Lett. **87**, 153902 (2001).
[8] J. J. Larsen, K. Hald, N. Bjerre, H. Stapelfeldt, and T. Seideman, Three dimensional alignment of molecules using elliptically polarized laser fields, Phys. Rev. Lett. **85**, 2470 (2000).
[9] H. Stapelfeldt and T. Seideman, Colloquium: aligning molecules with strong laser pulses, Rev. Mod. Phys. **75**, 543 (2003).
[10] S. Fleischer, Y. Khodorkovsky, E. Gershnabel, Y. Prior, and I. S. Averbukh, Molecular alignment induced by ultrashort laser pulses and its impact on molecular motion, Isr. J. Chem. **52**, 414 (2012).
[11] A. S. Chatterley, B. Shepperson, and H. Stapelfeldt, Three-dimensional molecular alignment inside helium nanodroplets, Phys. rev. Lett. **119**, 073202 (2017).
[12] J. Qiang, L. Zhou, P. Lu, K. Lin, Y. Ma, S. Pan, C. Lu, W. Jiang, F. Sun, W. Zhang, H. Li, X. Gong, I. S. Averbukh, Y. Prior, C. A. Schouder, H. Stapelfeldt, I. N. Cherepanov, M. Lemeshko, W. Jäger, and J. Wu, Femtosecond rotational dynamics of D_2 molecules in superfluid helium nanodroplets, Phys. Rev. Lett. **128**, 243201 (2022).
[13] A. A. Milner, V. A. Apkarian, and V. Milner, Dynamics of molecular rotors in bulk superfluid helium, Sci. Adv. **9**, eadi2455 (2023).
[14] J. Ma, H. Zhang, B. Lavorel, F. Billard, E. Hertz, J. Wu, C. Boulet, J.-M. Hartmann, and O. Faucher, Observing collisions beyond the secular approximation limit, Nature Commun. **10**, 5780 (2019).

[15] M. Bournazel, J. Ma, F. Billard, E. Hertz, J. Wu, C. Boulet, J. M. Hartmann, and O. Faucher, Non-markovian collisional dynamics probed with laser-aligned molecules, Phys. Rev.A **107**, 023115 (2023).

[16] M. Lapert, E. Hertz, S. Guérin, and D. Sugny, Field-free permanent molecular planar alignment, Phys. Rev. A **80**, 051403(R) (2009).

[17] M. Z. Hoque, M. Lapert, E. Hertz, F. Billard, D. Sugny, B. Lavorel, and O. Faucher, Observation of laser-induced field-free permanent planar alignment of molecules, Phys. Rev. A **84**, 013409 (2011).

[18] S. Gerstenkorn and P. Luc, Atlas du spectre d'absorption de la molecule d'iode, 14800-20000 cm^{-1} (Centre national de la recherche scientifique,1978).

[19] E. F. Thomas, A. A. Sondergaard, B. Shepperson, N. E. Henriksen, and H. Stapelfeldt, Hyperfine-structure-induced depolarization of impulsively aligned I_2 molecules, Phys. Rev. Lett. **120**, 163202 (2018).

[20] J. Tellinghuisen, Transition strengths in the visible-infrared absorption spectrum of I_2, J. Chem. Phys. **76**, 4736 (1982).

[21] J. Tellinghuisen, Intensity factors for the I_2 B-X band system, J. Quant. Spectrosc. Radiat. Transfer **19**, 149 (1978).

[22] J. T. Hougen, The calculation of rotational energy levels and rotational line intensities in diatomic molecules, US. Natl. Bur. Stds. Monograph **115** (1970).

[23] D. W. Broege, R. N. Coffee, and P. H. Bucksbaum, Strong-field impulsive alignment in the presence of high temperatures and large centrifugal distortion, Phys. Rev. A **78**, 035401 (2008).

[24] S. Ramakrishna and T. Seideman, Intense laser alignment in dissipative media as a route to solvent dynamics, Phys. Rev. Lett. **95**, 113001 (2005).

[25] M. Gruebele, G. Roberts, M. Dantus, R. M. Bowman, and A. H. Zewail, Femtosecond temporal spectroscopy and direct inversion to the potential: Application to iodine, Chem. Phys. Lett. **166**, 459 (1990).

[26] D. M. Willberg, J. J. Breen, M. Gutmann, and A. H. Zewail, Rotational constants of vibrationally excited iodine from purely rotational coherence observed in pump-probe experiments, J. Chem. Phys. **95**, 7136 (1991).

[27] H. Katsuki, H. Chiba, B. Girard, C. Meier, and K. Ohmori, Visualizing picometric quantum ripples of ultrafast wave-packet interference, Science **311**, 1589 (2006).

[28] R. Dörner, V. Mergel, L. Spielberger, O. Jagutzki, M. Unverzagt, W. Schmitt, J. Ullrich, R. Moshammer, H. Khemliche, M. Prior, R. E. Olson, L. Zhaoyuan, W. Wu, C. L. Cocke, and H. Schmidt-Böcking, Cold target recoil ion momentum spectroscopy, AIP Conference Proceedings **360**, 495 (1996).

[29] J. Wu, A. Vredenborg, B. Ulrich, L. P. H. Schmidt, M. Meckel, S. Voss, H. Sann, H. Kim, T. Jahnke, and R. Dörner, Nonadiabatic alignment of van der waals–force-bound argon dimers by femtosecond laser pulses, Phys. Rev. A **83**, 061403(R) (2011).

[30] S. Gerstenkorn, P. Luc, and J. Sinzelle, Study of the iodine absorption spectrum by means of fourier spectroscopy in the region 12 600-14000 cm^{-1}, J. Phys. France **41**, 1419 (1980).